A SIC Based BS Coordination Scheme for Full Duplex Cellular Networks

Hernán-Felipe Arraño-Scharager, Marceau Coupechoux, and Jean-Marc Kelif

Abstract—**Full Duplex (FD) in cellular networks is expected to increase the cell spectral efficiency. However, while the downlink (DL) spectral efficiency (SE) increases with FD, the uplink (UL) SE decreases because of the Base Station to Base Station (BS) interference. In this paper, assuming a three-node model, we propose a method based on Successive Interference Cancellation (SIC) to reduce the BS-to-BS interference present in FD cellular networks. The approach consists in coordinating BSs to enable the decoding and the suppression of undesired signals that impair uplink transmissions. We analyze both distributed and Centralized Radio Access Networks (CRAN) architectures. Stochastic geometry is used to derive the coverage probability and mean data rate of the proposed scheme. In the distributed scenario, the FD UL average data rate is increased by** 25% **with our solution compared to a classical FD network, while our FD scheme still outperforms Half-Duplex (HD) on the DL. In the centralized scenario, our solution outperforms HD by** 10% **and classical FD by** 78% **on the UL, while preserving classical FD gains on the DL.**

Index Terms—**5G; Full-Duplex; SIC; Base station coordination; Stochastic Geometry**

I. INTRODUCTION

Full-duplex (FD) enables a transceiver to simultaneously receive and transmit data in a given frequency band and time slot[1]. Assuming perfect self-interference cancellation (self-IC), FD can potentially double the spectral efficiency (SE) of a given point-to-point communication. This makes FD an appealing candidate to be implemented in BSs of next-generation wireless networks. If User Equipments (UE) are not able to perform FD, FD BSs are capable of simultaneously receiving data from a UE on the UL and transmitting data to another UE on the DL: This is known as the three-node model.

However, in this cellular network context, imperfect self-IC and co-channel interference restrict the expected gains of FD in terms of SE and prevent link data rates to achieve their theoretical upper bound. Nevertheless, several results show that when compared to traditional half-duplex (HD) cellular systems, FD implementation may enhance the overall per-cell SE [2]–[4]. The whole gain is however captured by the DL SE, while the UL SE suffers from a severe degradation [5], [6]. When FD is implemented in BSs, the additional interference

seen by a UE on the DL is compensated by the additional radio resource that are made available by the FD transmission. On the contrary, the UL suffers from Residual Self-Interference (RSI) after self-IC [7]. In addition, neighboring BSs, which are transmitting with high power compared to UEs create a huge co-channel interference that degrades the UL performance. As a consequence, FD is mostly envisioned in the literature for small cells (SCs) because of their low transmit power and favorable inter-BSs propagation conditions [8].

A promising approach to cope with UL interference is Successive Interference Cancellation (SIC), which allows a receiver (e.g. a BS) to successively cancel the co-channel interference before decoding the desired signal. This technique is performed for example to realize Non-Orthogonal Multiple Access (NOMA) but can be also used to suppress the interference from other BSs. SIC can be achieved for example by performing superposition coding [9]. In this paper, we propose and analyze a novel method, which builds upon the idea that BSs coordinate their transmissions and perform SIC to improve the Signal-to-Interference plus Noise Ratio (SINR) on the UL of FD cellular networks. The solution enhances the overall UL performance while flexibly limiting the DL gain if necessary. The performance evaluation is analytically derived using stochastic geometry tools and the numerical results in various scenarios show the expected gains of our approach.

A. Related Works

A set of papers in the literature try to tackle the UL interference problem by proposing hybrid solutions that combine HD and FD transmissions depending on the radio conditions or the locations of the interferers [2], [5], [10]. Hybrid in-band and out-of-band FD solutions are also proposed in [11], [12] for integrated access and backhaul, and machine-type communications respectively. Particularly, authors in [5] propose a duplex-switching policy for BSs based on the position of the scheduled users to directly reduce the UL degradation without considerably affecting the gains observed in FD DLs. Similarly, in [2], users decide the duplex-mode based on the received power from their serving BSs. All hybrid-duplex approaches prevent BSs to use FD when the served users are in unfavorable UL radio conditions. This results in a global reduction of the inter-cell interference level and hence an increase of the sum data rate, with respect to both traditional FD- and HD-systems. In [4], the authors propose and study an adjustable partial overlap between UL and DL signals. Here again, the result is to balance the trade-off between favorable DL gains and severely degraded ULs.

In all these works, the FD technique is restrained, and thus not fully exploited, with the goal of reducing uplink interference.

Another approach to reduce the co-channel interference in FD-based networks is to operate in the millimeter waves (mmW). Results in [13] show that FD-based systems using mmW can be jointly beneficial for DL and UL. As expected, DL benefits from the gains brought by FD, while UL takes advantage of a very low inter-BS interference due to the combined effect of high frequency and thin beamforming (see also [14], [15] for the effect of antenna directivity). Yet, the question of the efficiency of FD in lower bands remains open.

SIC has been studied for several years in the literature of cellular networks in order to allow multi-user transmissions on the same radio resource, see e.g. [16], [17]. Only recently, this technique has been proposed in conjunction with FD. In particular, NOMA is a promising technique to manage the additional interference experienced in FD-based networks [18]–[24]. In [18], the authors show the superiority of FD-NOMA over HD-NOMA but insist on the necessity to reduce co-channel interference. In [19], [20], the authors focus on a single cell and try to reduce interference at the DL user. Reference [21] tackles the problem of cross-tier interference, again on the DL. In several studies, FD-NOMA is envisioned at relays or for device-to-device communications [22]–[24]. These works consider SIC as a means to multiplex users, while the technique could also be used to mitigate inter-BS interference. SIC has been also used in conjunction with FD in [15], [25], [26], however with different network models and without considering the UL rate degradation issue. In the literature, SIC is preferably used at the UE, while BS capabilities are higher and BS-to-BS communication is arguably easier to achieve. To the best of our knowledge, there is no solution available to directly mitigate the BS-to-BS interference and, thus, directly attack the UL degradation experienced in traditional FD-based networks.

B. Contributions

In this paper, our main contribution is a BS coordination scheme for FD cellular networks, in which part of the UL co-channel interference is cancelled using SIC. To be more precise:

- We propose a novel method based on the principle of SIC to reduce the BS-to-BS interference present in FD-based cellular networks. The solution can be implemented in distributed, as well as in centralized architectures. In the distributed architecture, every BS first builds a set of its stronger UL interferers. Then, interferers adapt their data rate towards their DL user in order to allow SIC at the considered BS. When a UL transmission occurs, the BS can suppress part of the co-channel interference. In the centralized architecture, interference sets and SIC are handled by a central unit. To the best of our knowledge, this is the first method proposed to directly mitigate the BS-to-BS interference in FD cellular networks.
- We analyze the performance of our approach at the network level using stochastic geometry and propose closed-form equations for the coverage probability and average link data rates on the UL, DL and between BSs. Compared to the literature in stochastic geometry for cellular networks, new formulas are indeed required to stick to the novelty of the model.
- We show that our approach enhances FD ULs, while also outperforming HD DLs. With a distributed architecture, the solution enhances the mean UL data rate of FD networks by 25% and holds the DL gains experienced by typical FD systems, i.e., it increases the mean DL rate of HD networks by 49%. With a centralized architecture, the gains of FD on the DL are retained and our solution outperforms both HD and FD ULs by 10% and 78%, respectively.

The paper is organized as follows. In Section II, the system model is introduced. In Section III, the proposed method and algorithm are described. Section IV shows the derivation of the analytical performance by using stochastic geometry. Section V shows numerical results and system design insights are provided. Finally, Section VI concludes the paper.

II. SYSTEM MODEL

A. Network Model

We consider a cellular network in which BSs locations are modeled by a homogeneous Poisson Point Process (PPP)[2], Φ, of spatial density λ on $\mathbb{R}^2$. We denote $R_c = 1/\sqrt{\pi\lambda}$ the average cell radius in this network. Active UEs are attached to their closest BS. The network can thus be seen as a Voronoi tessellation of the network area, in which the coverage region of each BS is represented by its Voronoi cell. As in [27], [28], we assume that the density of active UEs is large with respect to λ. We assume that BSs operate in FD-mode, while UEs are in HD-mode[3]. As a consequence, every BS performs self-IC and transmissions result in Residual Self-Interference (RSI) at its own receiver.

Let Ω be the set of Resource Blocks (RB) over the system bandwidth W during one radio frame, every RB has a bandwidth of ω. As a worst case scenario, we consider a full buffer traffic model, a classical assumption in stochastic geometry [30], [31]: In every cell, there is always at least one UL and one DL active user. Among the UL (resp. DL) active users attached to a BS, one is randomly *scheduled* on every RB $\iota \in \Omega$. We can thus define two point processes $\Psi_u^{(\iota)}$ and $\Psi_d^{(\iota)}$ of *scheduled* UL and DL users, resp., in RB $\iota \in \Omega$. These processes are dependent on Φ and a realization can be obtained by drawing uniformly two points in every Voronoi cell of Φ. Therefore, by construction, $\Psi_u^{(\iota)}$ and $\Psi_d^{(\iota)}$ have the same intensity as Φ. As they are drawn from the same point process of active users, there are also inter-dependent. We make however the simplifying assumption that they are independent, as it is done e.g. in [4], [27], [32]. As all RBs are statistically equivalent, we now omit in the notation the

---

[2]We adopt stochastic geometry for the performance evaluation. The analysis will provide average data rates, specific deployments may lead to different performance depending on the random variable realizations, e.g. node locations.

[3]This model is known as the "three-node" model and is arguably realistic given the great difficulty to implement FD in user terminals [8], [29].

TABLE I
NOTATIONS.

Symbol	Definition	Symbol	Definition
Φ	Point process of BSs	λ	Spatial density of Φ
u, d, b	UL, DL and BS-to-BS link	Ψ_m	Process of scheduled UEs, $m \in \{u, d\}$
R_c	Average cell radius	P_d, P_u	BS and UE transmit powers
$G_{\max}, G_{\min}$	BS main- and side-lobe gains	G'	BS to UE in another cell net average gain
G	BS to scheduled UE net average gain	κ, η	BS to scheduled UE path-loss parameters
$\breve{G}$	Net average gain between BSs	$\breve{\kappa}, \breve{\eta}$	BS-to-BS path-loss parameters
$\tilde{G}$	Net average gain between UEs	$\tilde{\kappa}, \tilde{\eta}$	UE-to-UE path-loss parameters
G_{RSI}	Self-interference net average gain	$d(q, q')$	Distance between q and q'
$L(q, q')$	Distance dependent loss between q and q'	$h(q, q')$	Fast fading between q and q'
L_0	UE to serving BS path-loss	R_0	UE to serving BS distance
x, y	BS and UE position	$\gamma_m(q, q')$	SINR between q and q', $m \in \{u, d, b\}$
$I_{\text{BS}}^{(m)}$	Interference from BSs in link $m \in \{u, d\}$	$I_{\text{UE}}^{(m)}$	Interference from UEs in link $m \in \{u, d\}$
$\gamma_b^{(n)}$	SINR bw. a typical BS and the n-th closest BS	$I_{\text{BS}}^{(n)}$	Interference from other BSs in $\gamma_b^{(n)}$
$\mathcal{R}_m(x)$	Link data rate for BS in x, $m \in \{u, d\}$	$\mathcal{C}_m$	Instantaneous channel capacity, $m \in \{u, d, b\}$
$\mathcal{C}_b^{(n)}$	Instantaneous capacity for $\gamma_b^{(n)}$	$\mathcal{U}(x)$	BSs that x can decode to perform SIC
$I_M(x)$	Set of M strongest interferers of BS x	$J(x)$	BSs for which x is a strong interferer
$1 - \nu^\star$	Maximum allowed DL rate loss	R_M	Typical BS to M-th neighboring BS distance
f_R	Probability density function of RV R	$\mathscr{L}\{X\}(s)$	Laplace transform of RV X
$\mathcal{P}_m$	Coverage probability for $m \in \{u, d\}$	$\mathcal{P}_b^{(n)}$	Coverage probability for $\gamma_b^{(n)}$
$p(r)$	Probability that a typical BS cannot decode/suppress a BS at a distance r	M	Maximum number of BSs that can be decoded using SIC

dependence on ι, and without loss of generality we write $\Psi_m^{(\iota)}$ as Ψ_m, $m \in \{u, d\}$. The notations of the paper are summarized in Tab. I.

B. Transmission and Propagation Model

UEs and BSs transmit powers are denoted P_u and P_d, respectively. Users have omnidirectional antennas, with an antenna gain of $G_u = 1$. We adopt a side-lobe and main-lobe model [13], [33] for BSs, with antenna gains $G_{\min}$ and $G_{\max}$, respectively, see Fig. 1a. The beamwidth of the main-lobe is characterized by the angle $\theta_{3\text{dB}}$. Hence, the side-lobe of gain $G_{\min}$ covers the angle $2\pi - \theta_{3\text{dB}}$. Every BS steers two main lobes in the direction of its scheduled UL and DL UE, respectively[4]. Accordingly, we assume the following net average antenna gains between network equipments: $G \triangleq G_{\max}G_u$, between a BS and a scheduled UE; $\breve{G}$, between two BSs; G', between a BS and a UE scheduled by another cell; $\tilde{G} \triangleq G_u^2$, between two UEs; G_{RSI} for the self-interference between the transmitter of a FD BS and its own receiver. $\breve{G}$ and G' are computed using the probabilities of being in the direction of a side-lobe $p_s = (2\pi - \theta_{3\text{dB}})/(2\pi)$ or a main lobe $1 - p_s$ assuming random uniform directions. For the BS transceiver, since it simultaneously receives and transmits, the RSI gain is the result from the interference between the lobes pointing the DL and UL users, i.e., $G_{\text{RSI}} = p_s^2 G_{\max}G_{\min} + (1 - p_s^2)G_{\max}^2$. This gain accounts for the direct path between the transmit and receive antennas. In the three-node model, passive self-interference suppression is indeed achieved when the difference between the pointing directions of the transmit and receive antennas is sufficiently large [34].

Let the channel loss between two locations q and q' be $\ell(q, q') = L(q, q')/h(q, q')$, where $L(q, q') = (K d(q, q'))^\alpha$ is the deterministic distance dependent path-loss, $d(q, q')$ is

the distance between q and q', K is the link reference path-loss at 1 meter, α is the path-loss exponent and $h(q, q')$ is an exponential random variable (RV) with mean 1 that models fast fading between q and q' [33], [35]. In the sequel, we assume that: $K = \kappa$ and $\alpha = \eta$, for the channel between a BS and a scheduled UE; $K = \breve{\kappa}$ and $\alpha = \breve{\eta}$, for the channel between two BSs; $K = \tilde{\kappa}$ and $\alpha = \tilde{\eta}$, for the channel between two UEs. The propagation parameters are illustrated in Fig. 1b. For a typical user located in 0, we denote $L_0 = (\kappa R_0)^\eta$ the deterministic path-loss to its serving BS in x, where $R_0 = \min_{x' \in \Phi} d(0, x')$. When referring to a typical user or a typical BS and when the context is clear, we write $d(x) = d(0, x)$, $h(0, x) = h(x)$ and $L(0, x) = L(x)$.

C. SIC Model

In a power domain SIC transmission [36, Chapter 6], a set $\tilde{\mathcal{U}}$ of transmitters transmit signals to a common receiver on the same radio resource. At the receiver, SIC is performed to retrieve each transmitted information. The SIC decoder is characterized by a decoding order, i.e., a permutation function $\pi : \tilde{\mathcal{U}} \to \tilde{\mathcal{U}}$. For $i \in \tilde{\mathcal{U}}$, $\pi(i)$ represents the i-th decoded transmitter, and conversely the order at which transmitter q is decoded is given by $\pi^{-1}(q)$. Consequently, the i-th decoded signal is only subject to interference coming from transmitters $\pi(j)$, such that $j > i$. For the medium access channel, there is no constraint on the choice of π if we do not require to be on the capacity region border. An example of decoding order would be to decode starting from the strongest transmitter first and move towards the weakest transmitter. In our solution, the receiver is a BS and the set of transmitters is made of an uplink user and the strongest interfering BSs. Using SIC, the interfering BSs are decoded first and the UL user signal is decoded last.

---

[4]This can be achieved by using a hybrid implementation of massive MIMO with two RF chains and two antenna panels.

(a) Main and side-lobe model.

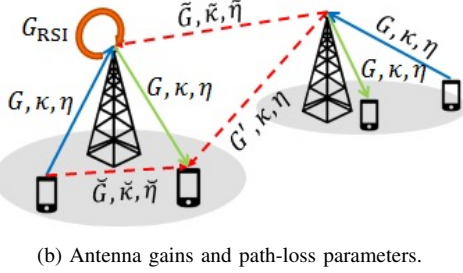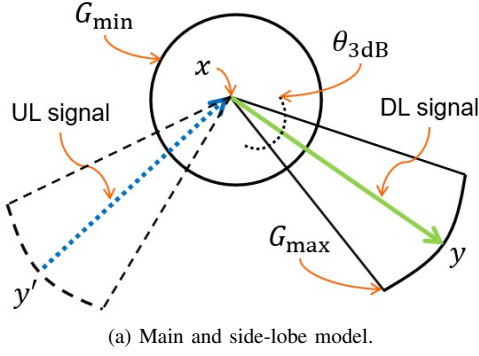(b) Antenna gains and path-loss parameters.

Fig. 1. Antenna and propagation parameters. (a) The BS located in x, is transmitting towards a DL user in y, while receiving data from an UL user in y'. (b) Propagation parameters and net antenna gains depends on the equipments.

D. SINR Formulations

1) DL SINR: We denote $\gamma_d(x,y)$ the DL SINR of a user located in y and served by a BS in x; it can be written as:

$$\gamma_d(x,y) = \frac{GP_d h L(x,y)^{-1}}{I_{\mathrm{BS}}^{(d)}(x,y) + I_{\mathrm{UE}}^{(d)}(y) + \sigma^2}, \tag{1}$$

where $I_{\mathrm{BS}}^{(d)}(x,y) = \sum_{x' \in \Phi \setminus \{x\}} G' P_d h(x',y) L(x',y)^{-1}$, is the interference coming from other BSs, $I_{\mathrm{UE}}^{(d)}(y) = \sum_{y' \in \Psi_u} \tilde{G} P_u h(y,y') L(y,y')^{-1}$, is the interference from UL users, and σ^2 is the thermal noise power. When y is the typical DL user, we write $\gamma_d^{(0)} \triangleq \gamma_d(x,0)$, $I_{\mathrm{BS}}^{(d)} \triangleq I_{\mathrm{BS}}^{(d)}(x,0)$, $I_{\mathrm{UE}}^{(d)} \triangleq I_{\mathrm{UE}}^{(d)}(0)$, where x is the closest BS to y.

2) UL SINR: Let us consider a BS in x serving an UL user in y and assume that the BS is able to successively suppress the interference from a set $\mathcal{U}$ of neighboring BSs. The set $\tilde{\mathcal{U}} = \mathcal{U} \cup \{y\}$ defined in Section II-C is now formed by the UL user and the neighboring BSs in $\mathcal{U}$. In this setting, the UL user is the last one to be decoded, i.e., $\pi(y) > \pi(i)$ for all $i \in \mathcal{U}$. This choice does not necessarily achieves the capacity region border; it is however the optimal choice for the UL user. For this user, we define the UL SINR at the BS, $\gamma_u(y,x)$, as:

$$\gamma_u(y,x) = \frac{GP_u h(y,x) L(y,x)^{-1}}{I_{\mathrm{BS}}^{(u)}(y,x;\mathcal{U}) + I_{\mathrm{UE}}^{(u)}(y,x) + I_{\mathrm{RSI}} + \sigma^2}, \tag{2}$$

where

$$I_{\mathrm{BS}}^{(u)}(y,x;\mathcal{U}) = \sum_{x' \in \Phi \setminus \{\{x\} \cup \mathcal{U}\}} \breve{G} P_d h(x',x) L(x',x)^{-1} \tag{3}$$

is the interference coming from other BSs at BS y, $I_{\mathrm{UE}}^{(u)}(y,x) = \sum_{y' \in \Psi_u \setminus \{y\}} G' P_u h(y',x) L(y',x)^{-1}$ is the interference from other scheduled UL users and I_{RSI} is the RSI

power given by $I_{\mathrm{RSI}} = \beta\, G_{\mathrm{RSI}} P_d$, where $\beta \in [0,1]$ is a constant related to the performance of the self-IC used at the BS receiver. A constant factor for the self-IC capability is widely used in the literature, see e.g. [2], [3], [8]. When x is the typical BS, we write $\gamma_u^{(0)} \triangleq \gamma_u(y,0)$, $I_{\mathrm{BS}}^{(u)}(\mathcal{U}) \triangleq I_{\mathrm{BS}}^{(u)}(y,0;\mathcal{U})$, $I_{\mathrm{UE}}^{(u)} \triangleq I_{\mathrm{UE}}^{(u)}(y,0)$, where y is the scheduled UE.

3) BS-to-BS SINR: For our proposed scheme, we need to define the BS-to-BS SINR for a transmission occurring from a BS x' to a BS x. The BS-to-BS SINR is given by:

$$\gamma_b(x',x) = \frac{\breve{G} P_d h(x',x) L(x',x)^{-1}}{I_{\mathrm{BS}}(x',x) + I_{\mathrm{UE}}(x) + I_{\mathrm{RSI}} + \sigma^2}, \tag{4}$$

where

$$I_{\mathrm{BS}}(x',x) = \sum_{x'' \in \Phi \setminus \{x,x'\}} \breve{G}\, P_d h(x'',x) L(x'',x)^{-1} \tag{5}$$

is the interference from all other BSs and $I_{\mathrm{UE}}(x) = \sum_{y \in \Psi_u} G' P_u h(y,x) L(y,x)^{-1}$ the one from UL users. When x is the typical BS, we write $\gamma_b^{(0)}(x') \triangleq \gamma_b(x',0)$. When x is the typical BS and x' is its n-th closest BS, $n \in \mathbb{N}$, we write $\gamma_b^{(n)} \triangleq \gamma(x',0)$, $I_{\mathrm{BS}}^{(n)} \triangleq I_{\mathrm{BS}}(x',0)$, and $I_{\mathrm{UE}}^{(b)} \triangleq I_{\mathrm{UE}}(0)$.

E. Coverage Probability, Capacity and Rate

The coverage probability for a link $m \in \{u,d,b\}$ is given by $\mathbb{P}(\gamma_m > \tau)$, where τ is a threshold.

The instantaneous link capacity is defined using the Shannon's formula: $\mathcal{C}_m = \omega \log_2 (1 + \gamma_m)$. In particular, on the UL, the capacity depends on the set $\mathcal{U}$ of BSs whose interference can be suppressed and we explicitly write $\mathcal{C}_u(\mathcal{U})$. The ergodic capacity with receiver channel side information (CSI), i.e., the Shannon capacity averaged over the distribution of γ_m for $m \in \{u,d,b\}$, is given by [37, Chapter 4]: $\bar{\mathcal{C}}_m = \mathbb{E}_{\gamma_m}[\omega \log_2 (1 + \gamma_m)]$. Capacity expressions provide upper bounds for the achievable data rates on a given link.

We denote $\mathcal{R}_m$ the actual data rate chosen on link m and we have[5] that $\mathcal{R}_m \leq \mathcal{C}_m$. In the following, we may omit the location of the scheduled user and write $\mathcal{R}_m(x) = \mathcal{R}_m(x,y)$, $m \in \{u,d\}$, when it is clear from the context.

III. SIC BASED BS COORDINATION SCHEME

A. Algorithm

Our goal is to minimize as much as possible the impact of $I_{\mathrm{BS}}^{(u)}$ on the UL performance. In a nutshell, our solution builds upon the following idea: Every BS attempts to decode and suppress the signal of the main co-channel interferers. A BS i is able to suppress the signal from an interfering BS j only if the data rate of j towards its DL user is less than the channel capacity between i and j. If it is not the case, we may decide to decrease the data rate of j below the capacity between i and j. Algorithm 1 shows the proposed approach in details.

For a BS $x \in \Phi$, we proceed as follows:

---

[5]In theory, any arbitrary data rate can be chosen strictly less than the capacity. In practice, a finite set of data rates are achievable. For simplicity, in this paper, we assume a continuous set of available data rates less or equal to the link capacity.

Algorithm 1 SIC Based BS Coordination Scheme (run at BS x)

1: **Input**: Φ, M, $\nu^\star$
2: **Output**: $\mathcal{R}_d(x)$, $\mathcal{R}_u(x)$
3: **Init**: $J(x; M) \leftarrow \emptyset$
4: $I_M(x) \leftarrow$ BSs with the M smallest path-losses $L(x, x')$, $x' \in \Phi$
5: $I_M(x) \leftarrow \text{SORT}(I_M(x))$
6: Send message to BSs in $I_M(x)$
7: **for** Every message received from x'' **do**
8: $\quad J(x; M) \leftarrow J(x; M) \cup \{x''\}$
9: $\quad$ Estimate $h(x, x'')$
10: $\quad$ Estimate $\mathcal{C}_b(x, x'')$ $\qquad \triangleright$ using the estimation of $h(x, x'')$ and (4)
11: **end for**
12: Estimate $\mathcal{C}_d(x)$ $\qquad \triangleright$ using DL SINR expression (1)
13: $\mathcal{C}_{\min}(x; M) \leftarrow$ (6)
14: $\nu(x) \leftarrow$ (8)
15: $\mathcal{R}_d \leftarrow$ (7)
16: $\mathcal{U}(x) \leftarrow$ (9) $\qquad \triangleright$ using $\mathcal{R}_d(x')$, $x' \in I_M(x)$
17: $\mathcal{R}_u(x) \leftarrow$ (10)
18: **return** $\mathcal{R}_d$, $\mathcal{R}_u$

1) Let $I_M(x)$ be the set of the M strongest interfering BSs averaging out fast fading[6] (step 4). M is the maximum number of interfering signals that can be suppressed using SIC. It depends on the performance of the SIC implementation and is an input of our algorithm. $I_M(x)$ is the set of BSs that x can potentially decode using SIC if their data rate is less than the capacity towards x. With our channel model, $I_M(x)$ is also the set of M closest BSs. Let $J(x; M)$ be the set of BSs for which x is a strong interferer, i.e., $J(x; M) = \{x'' \in \Phi \mid x \in I_M(x'')\}$ (step 8). The BS x can be potentially decoded by BSs in $J(x)$ if its data rate allows it. We estimate for every x'' the Shannon capacity between x and x'' (step 10). We define (step 13):

$$\mathcal{C}_{\min}(x; M) \triangleq \min_{x'' \in J(x; M)} \mathcal{C}_b(x, x'') \qquad (6)$$

If the data rate of x towards its DL user is less than $\mathcal{C}_{\min}$, all BSs in $J(x)$ are able to suppress x's signal; otherwise some BSs in $J(x)$ may not be able to decode x's signal.

2) BS x may adapt its DL data rate in order to be decodable at BSs in $J(x)$. In general, it chooses a DL rate as follows (step 15):

$$\mathcal{R}_d(x) = \nu(x) \mathcal{C}_d(x), \qquad (7)$$

where (step 14)

$$\nu(x) \triangleq \max\left(\min\left(\frac{\mathcal{C}_{\min}(x; M)}{\mathcal{C}_d(x)}, 1\right), \nu^\star\right) \qquad (8)$$

[6]Said differently, the measurements based on which this set is defined span over a period longer than the coherence time of the channel. Updating this set at the time-scale of the coherence-time would be too fast and seems thus unrealistic.
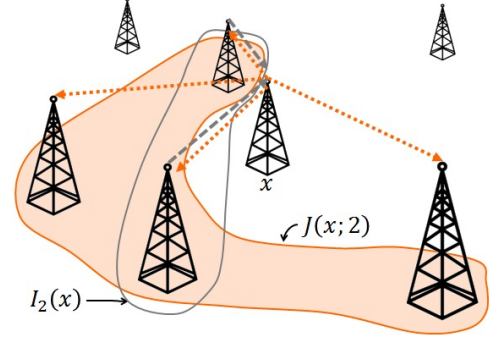

Fig. 2. Interference sets $I_M(x)$ and $J(x)$ for $M = 2$.

and $\nu^\star \in [0, 1]$ is a system parameter that characterizes the maximum DL rate and $1 - \nu^\star$ is the maximum loss factor tolerated by BS x on the DL. Note that the rate adaptation is performed using a different modulation and coding scheme and thus does not affect the transmit power. The process to set the DL rate is performed at every BS, in particular BSs in $I_M(x)$. We can thus now define $\mathcal{U}$ to be the set of BSs that can be decoded by x, i.e. (step 16),

$$\mathcal{U}(x) = \{x' \in I_M(x) \mid \mathcal{R}_d(x') \leq \mathcal{C}_b(x', x)\}. \qquad (9)$$

3) BS x chooses an UL rate as follows (step 17):

$$\mathcal{R}_u(x) = \mathcal{C}_u(x; \mathcal{U}(x)). \qquad (10)$$

In the sequel, when the context is clear we write $J(x) = J(x; M)$. Further, when x is the typical BS we write $\mathcal{R}_d^{(0)} \triangleq \mathcal{R}_d(0)$, $\mathcal{C}_d^{(0)} \triangleq \mathcal{C}_d(0)$ and $\mathcal{C}_{\min}^{(0)}(M) \triangleq \mathcal{C}_{\min}(0; M)$. Moreover, when the n-th neighbor of the typical BS located in x' is at a distance r, i.e. $d(0, x') = r$, then we write $\mathcal{C}_b^{(n)}(r) \triangleq \mathcal{C}_b^{(n)}(0, x')$, $\mathcal{C}_d(r) \triangleq \mathcal{C}_d(x')$ and $\mathcal{R}_d(r) \triangleq \mathcal{R}_d(x')$.

We see from the algorithm that the performance of our solution depends on the channel capacity between BSs. This is the reason why, we model in this paper the BS-to-BS wireless communication.

A graphical representation of the interference sets $I_M(x)$ and $J(x)$ for a BS $x \in \Phi$ is shown in Fig. 2. BSs inside the region covered by the gray-bold line are the two closest and stronger interferers of the BS in x, i.e., $I_2(x)$. The gray-dashed arrows represent their signals towards x, they can be cancelled by x using SIC if their respective DL rates are lower than the capacity between them and x. The BSs inside the orange region are the BSs that are strongly interfered by the BS x, given the value of M, i.e., $J(x; M)$. The orange-dotted arrows are the signals used by BSs in $J(x)$ to decide whether x is a strong interferer. A BS in $J(x)$ is able to cancel x's signal if the DL rate of x is less than the capacity along the orange arrow. The following remarks explain how (8) has been designed by considering some special cases.

Remark 1. *If $\mathcal{C}_{\min}(x) \geq \mathcal{C}_d(x)$, then BS x can be decoded by all BSs in $J(x)$, i.e., for which it is a strong interferer. In this case, there is no need to degrade the DL rate of BS x to allow SIC at the BSs it interferes, so that $\nu(x) = 1$ and $\mathcal{R}_d(x) = \mathcal{C}_d(x)$ in (7) and (8).*

Remark 2. *If $\mathcal{C}_{\min}(x) < \mathcal{C}_d(x)$, BS x can choose to degrade its DL rate to be decoded by the BSs it interferes. The higher the degradation, the higher the number of BSs that will be able to suppress x. In this regard, $1 - \nu^\star$ sets a maximum tolerable DL rate degradation. If additionally $\mathcal{C}_{\min}(x)/\mathcal{C}_d(x) \geq \nu^\star$, x can set its DL rate to $\mathcal{C}_{\min}(x)$ and still be decoded by all BSs in $J(x)$.*

Remark 3. *On the UL, the capacity depends on the ability of BS x to suppress the interference from BSs in $I_M(x)$ and, thus, depends in (10) on the set $\mathcal{U}(x)$. This set indeed includes BSs of $I_M(x)$ whose DL rate (adjusted by $\nu^\star$) is less than the capacity towards x.*

Remark 4. *When $\nu^\star = 0$, BSs accept any degradation on the DL. Thus, $\mathcal{R}_d(x') \leq \mathcal{C}_b(x', x)$. As a consequence, $|\mathcal{U}(x)| = M$ and the M strongest interferers can be suppressed.*

The complexity of Algorithm 1 is dominated by the sorting of step 5 in $O(M \log M)$ and the channel estimation performed at every received message, which is typically in $O(N^3)$ assuming OFDM MMSE channel estimation with Discrete Fourier Transform of size N. The overall complexity is thus in $O(N^3 M + M \log M)$ and the algorithm involves the transmission of M new signalling messages at every run, which is reasonable for the practical values of M we consider in this paper (less than 10). Note that if the BS-to-BS capacity is under-estimated in step 10, SIC can still be performed but the reduction of DL data rate (if applied) could be too drastic. If this capacity is over-estimated, SIC may not be performed implying a reduction of the UL data rate.

B. Network Topology

Our algorithm can be implemented in a distributed or centralized manner. In both cases, channel estimation (step 9) is based on typical pilot signals broadcast by every BS. The message sent by a BS in step 6 shall thus include pilots and the BS identity. At every BS, it is sent on dedicated DL radio resources that are excluded from the full duplex operation.

1) Distributed Architecture: BSs are directly connected between them through a wired transport network used to discover interfering BSs. In this scenario, the algorithm and the data processing are run at every BS, as suggested by Algorithm 1. The distributed approach allows a simplified architecture because it does not involve any new equipment. It is scalable in the sense that the amount of calculations and message exchanges depends locally only on M. SIC decoding is performed locally and thus with no additional delay. However, it requires additional computation capability at every BS and computation power cannot be mutualised. When new BSs are added or existing BSs are suppressed, this should be discovered by neighboring BSs[7].

2) Centralized Architecture: Under a Centralized Radio Access Network (CRAN) topology, a central unit (CU) manages the different BSs in a given area and runs the proposed algorithm on behalf of them. Since all the information is

gathered at the CU, steps 7 to 11 are bypassed. Therefore, $\mathcal{C}_b(x, x'')$ in step 10 can be set as: $\mathcal{C}_b(x, x'') \to +\infty$, $\forall x \in \Phi$ and $x'' \in I_M(x)$. This implies that $\nu(x) = 1$, for every BS (i.e., there is no need to degrade the DL rate). Moreover, since the processing is done at the CU, BSs can cancel the interference from all M BSs in $I_M(\cdot)$. A CRAN architecture reduces the amount of signalling as BSs communicate only with the CRAN. Processing powers can be mutualised. Any update in the number of BSs is easily taken into account by the algorithm. Among the drawbacks, an additional equipment is required and the communication between two neighboring CRANs should be managed. At last, the processing at the CRAN implies a delay that could be incompatible with low latency services. The analysis developed in the next section is valid for CRAN implementation provided that $\mathcal{C}_b(x, x'') \to +\infty$.

IV. ANALYTICAL PERFORMANCE ANALYSIS

A. Coverage Probabilities

1) Dowlink Coverage Probability:

Theorem 1 (Downlink coverage probability). *The DL coverage probability of a typical user, $\mathcal{P}_d(\tau) \triangleq \mathbb{P}(\gamma_d^{(0)} > \tau)$, is given by:*

$$\mathcal{P}_d(\tau) = \int_0^\infty f_{R_0}(r) \mathscr{L}\{I_{\mathrm{BS}}^{(d)}\}(r, \tau) \mathscr{L}\{I_{\mathrm{UE}}^{(d)}\}(r, \tau) N_d(r, \tau) \mathrm{d}r, \tag{11}$$

where $N_d(r, \tau) = \exp\left(-\tau(\kappa r)^\eta \sigma^2 (G P_d)^{-1}\right)$,

$$f_{R_0}(r) = 2(13/10)\pi r \lambda \exp\left(-(13/10)\lambda \pi r^2\right). \tag{12}$$

$\mathscr{L}\left\{I_{BS}^{(d)}\right\}$ *is given by* (13), $\mathscr{L}\left\{I_{UE}^{(d)}\right\}$ *by* (14), $\mu = P_u/P_d$ *and we further define $\mathscr{F}_d(r, \tau) \triangleq \mathscr{L}\{I_{\mathrm{BS}}^{(d)}\}(r, \tau) \mathscr{L}\{I_{\mathrm{UE}}^{(d)}\}(r, \tau) N_d(r, \tau).$*

Proof: See Appendix A. ∎

Remark 5. *Note that if $I_{\mathrm{UE}}^{(d)} = 0$ and $\mathscr{L}\{I_{\mathrm{UE}}^{(d)}\} = 1$, then* (11) *is exactly the DL coverage probability of a HD network, see e.g. [28]. If UEs are able to beamform their signal with a very thin beam towards their serving BS, $\tilde{G} \to 0$ with a high probability and, according to* (14), $\mathscr{L}\{I_{\mathrm{UE}}^{(d)}\} \to 1$. *This shows that omnidirectional UE antennas represent a worst case for FD. In the same way, when $\tilde{\eta} \to +\infty$, $\mathscr{L}\{I_{\mathrm{UE}}^{(d)}\} \to 1$.*

Corollary 1. *The probability density function (PDF) of $\gamma_d^{(0)}$ is given by $f_{\gamma_d^{(0)}}(\tau) \triangleq (\partial/\partial\tau) \mathbb{P}(\gamma_d^{(0)} \leq \tau) = (\partial/\partial\tau) 1 - \mathcal{P}_d(\tau)$, i.e., equation* (15).

2) BS-to-BS Coverage Probability:

Theorem 2 (BS-to-BS CCDF). *The complementary CDF (CCDF) of the SINR between a typical BS and its n-th closest interfering BS, i.e. $\mathcal{P}_b^{(n)}(\tau) \triangleq \mathbb{P}(\gamma_b^{(n)} > \tau)$, can be approximated by* (16), *where $N_b(r, \tau) \triangleq \exp\left(-\tau(\check{\kappa}r)^{\check{\eta}}(\check{G}P_d)^{-1}(I_{\mathrm{RSI}} + \sigma^2)\right)$,*

$$f_R(r, n) = \frac{2(\pi\lambda)^n}{(n-1)!} r^{2n-1} \mathrm{e}^{-\pi\lambda r^2}. \tag{17}$$

$$\mathscr{L}\left\{I_{\mathrm{BS}}^{(d)}\right\}(r,\tau) = \exp\left(-2\pi\lambda\int_r^\infty \left(1 - \exp\left(-\tau\frac{G'}{G}(r/z)^\eta\right)\right)z\mathrm{d}z\right), \tag{13}$$

$$\mathscr{L}\left\{I_{\mathrm{UE}}^{(d)}\right\}(r,\tau) = \exp\left(-2\pi\int_0^\infty \lambda_u(z)\left(1 - \exp\left(-\tau\mu\frac{\tilde{G}}{G}\frac{(\kappa r)^\eta}{(\tilde{\kappa}z)^{\tilde\eta}}\right)\right)z\mathrm{d}z\right), \tag{14}$$

$$f_{\gamma_d^{(0)}}(\tau) = \int_0^\infty f_{R_0}(r)\mathscr{F}_d(r,\tau)(\kappa r)^\eta \cdot \left[\frac{\sigma^2}{GP_d} + 2\pi\lambda\frac{G'}{G}\int_r^\infty \exp\left(-\tau\frac{G'}{G}(r/z)^\eta\right)\frac{z}{(\kappa z)^\eta}\mathrm{d}z\right.$$
$$\left. + 2\pi\lambda\mu\frac{\tilde{G}}{G}\int_0^\infty \exp\left(-\tau\mu\frac{\tilde{G}}{G}\frac{(\kappa r)^\eta}{(\tilde{\kappa}z)^{\tilde\eta}}\right)\frac{z}{(\tilde{\kappa}z)^{\tilde\eta}}\mathrm{d}z\right]\mathrm{d}r. \tag{15}$$

$$\mathcal{P}_b^{(n)}(\tau) = \int_0^\infty f_R(r,n)\mathscr{L}\{I_{\mathrm{BS}}^{(n,1)}\}(r,\tau)\mathscr{L}\{I_{\mathrm{BS}}^{(n,2)}\}(r,\tau)\mathscr{L}\{I_{\mathrm{UE}}^{(b)}\}(r,\tau)N_b(r,\tau)\mathrm{d}r, \tag{16}$$

$$\mathscr{L}\left\{I_{\mathrm{BS}}^{(n,1)}\right\}(r,\tau) = \left[\frac{2}{\breve{\eta}}\tau^{2/\breve\eta}\Gamma\left(-\frac{2}{\breve\eta},\tau\right)\right]^{n-1}, \tag{18}$$

$$\mathscr{L}\left\{I_{\mathrm{BS}}^{(n,2)}\right\}(r,\tau) =$$
$$\exp\left(-2\pi\lambda\int_r^\infty\left(1 - \exp\left(-\tau(r/z)^{\breve\eta}\right)\right)z\mathrm{d}z\right), \tag{19}$$

$$\mathscr{L}\left\{I_{\mathrm{UE}}^{(b)}\right\}(r,\tau) =$$
$$\mathbb{E}_{f_{R_0}}\left[\exp\left(-2\pi\lambda\int_0^{R_0}\left(1 - \exp\left(-\tau\mu\frac{G}{\breve{G}}\frac{(\breve\kappa r)^{\breve\eta}}{(\kappa z)^\eta}\right)\right)z\mathrm{d}z\right)\times\right.$$
$$\left.\exp\left(-2\pi\lambda\int_{R_0}^\infty\left(1 - \exp\left(-\tau\mu\frac{G'}{\breve{G}}\frac{(\breve\kappa r)^{\breve\eta}}{(\kappa z)^\eta}\right)\right)z\mathrm{d}z\right)\right]. \tag{20}$$

Additionally, we define $\mathscr{F}_b^{(n)}(r,\tau) \triangleq \mathscr{L}\{I_{\mathrm{BS}}^{(n)}\}(r,\tau)\mathscr{L}\{I_{\mathrm{UE}}^{(b)}\}(r,\tau)N_b(r,\tau)$ and $\mathscr{L}\{I_{\mathrm{BS}}^{(n)}\}(r,\tau) \triangleq \mathscr{L}\{I_{\mathrm{BS}}^{(n,1)}\}(r,\tau)\mathscr{L}\{I_{\mathrm{BS}}^{(n,2)}\}(r,\tau)$.

Proof: See Appendix B. ∎

3) Uplink Coverage Probability: To compute the UL coverage probability we proceed by assuming that the process of interfering BSs is a thinned PPP with intensity $\lambda p(r)$, where $p(r)$ is the probability that a typical BS is not able to decode and suppress the interference coming from another BS located at a distance r. We validate this assumption by simulations in Section V. To characterize $p(r)$, we observe that a BS at distance r from the typical BS is not decoded either if it is farther than the M-th closest BS (as a BS can only decode BSs in its set I_M) or if its DL rate $\mathcal{R}_d(r)$ is greater than the capacity between this BS and the typical BS, i.e:

$$p(r) = \mathbb{P}(r > R_M) + \mathbb{P}(r \le R_M \wedge \mathcal{R}_d(r) > \mathcal{C}_b(r)), \tag{21}$$

where R_M is the distance from a typical BS to its M-th neighboring BS. We have now the following results for the expression of $p(r)$.

Lemma 1. *If $\nu^\star = 0$, then:*

$$p(r) = 1 - \frac{\Gamma(M,\lambda\pi r^2)}{(M-1)!}. \tag{22}$$

In the general case, we have:

$$p(r) = \mathbb{P}(r > R_M) + \mathbb{P}(r \le R_M) \cdot$$
$$\sum_{n=1}^M \mathbb{P}\left(\nu^\star\mathcal{C}_d(r) > \mathcal{C}_b^{(n)}(r)\right) \cdot$$
$$P_1(M)\frac{(\lambda\pi r^2)^{(n-1)}}{(n-1)!}e^{-\lambda\pi r^2}, \tag{23}$$

where

$$\mathbb{P}\left(\nu^\star\mathcal{C}_d(r) > \mathcal{C}_b^{(n)}(r)\right) =$$
$$1 - \mathbb{E}_{\gamma_d^{(0)}}\left[\mathscr{F}_b^{(n)}\left(r,\left(1+\gamma_d^{(0)}\right)^{\nu^\star}-1\right)\right]. \tag{24}$$

and

$$P_1(M) = \mathbb{P}\left(\mathcal{C}_{\min}^{(0)}(M) \le \nu^\star\mathcal{C}_d^{(0)}\right) \tag{25}$$

Proof: See Appendix C ∎

The expectation in (24) can be computed using Corollary 1. The right hand side of (25) is derived in Section IV-C, equation (33).

Theorem 3 (UL Coverage Probability). *The UL coverage probability of a typical BS, $\mathcal{P}_u(\tau) \triangleq \mathbb{P}(\gamma_u^{(0)} > \tau)$, can be approximated by:*

$$\mathcal{P}_u(\tau) = \tag{26}$$
$$\int_0^\infty f_{R_0}(r)\mathscr{L}\left\{I_{\mathrm{BS}}^{(u)}(\mathcal{U})\right\}(r,\tau)\mathscr{L}\left\{I_{\mathrm{UE}}^{(u)}\right\}(r,\tau)N_u(r,\tau)\mathrm{d}r,$$

where $N_u(r,\tau) = \exp\left(-\tau(\kappa r)^\eta(GP_u)^{-1}(I_{RSI}+\sigma^2)\right)$, f_{R_0} is given by (12) and

$$\mathscr{L}\left\{I_{\mathrm{UE}}^{(u)}\right\}(r,\tau) = \tag{27}$$
$$\exp\left(-2\pi\int_0^\infty \lambda_u^{(BS)}(z)\left(1 - \exp\left(-\tau\frac{G'}{G}(r/z)^\eta\right)\right)z\mathrm{d}z\right),$$

$$\mathscr{L}\left\{I_{\mathrm{BS}}^{(u)}(\mathcal{U})\right\}(r,\tau) = \tag{28}$$
$$\exp\left(-2\pi\lambda\int_0^\infty p(z)\left(1 - \exp\left(-\tau\frac{\breve{G}}{G\mu}\frac{(\kappa r)^\eta}{(\breve\kappa z)^{\breve\eta}}\right)\right)z\mathrm{d}z\right),$$

where $p(z)$ is given by (23).

Proof: We approximate the process of interfering BSs by applying a $p(r)$-thinning rule to Φ. From this, we obtain (26) by following similar steps as for the proofs of Theorems 1 and 2. ∎

Remark 6. *For $\nu^\star = 0$, when $M \to \infty$, then $\mathbb{P}(r \leq R_M) \to 1$. Hence, $p(r) \to 0$, i.e., there is no BS-to-BS co-channel interference since for this scenario $\mathscr{L}\{I_{BS}^{(u)}(\mathcal{U})\}(r, \Gamma) = 1$ and we obtain the maximum performance for ULs.*

The UL coverage probability of Theorem 3 can be computed as soon as the distribution of $\mathcal{C}_{\min}(M)$ in $P_1(M)$ is available (see (25)). Given the technical difficulties to derive this distribution, we rely in the next section on an approximation.

B. Approximation of the Distribution of $\mathcal{C}_{\min}$

We assume that for a given value of M, $\mathcal{C}_{\min}^{(0)}(M) \approx \mathcal{C}_b^{(M')}$, where M' is an integer. This approximation is sustained by numerical observations and we will provide the mapping between M and M' in Section V for our simulation parameters.

C. Average Data Rates

Theorem 4 (Average DL rate). *The average DL data rate is given by:*

$$\mathbb{E}[\mathcal{R}_d] = \overline{\mathcal{C}}_{\min}^{(0)}(M)P_2(M) + \overline{\mathcal{C}}_d^{(0)}(\nu^\star P_1(M) + P_3(M)),$$
(29)

where

$$\overline{\mathcal{C}}_d^{(0)} \triangleq \omega\mathbb{E}\left[\log_2\left(1 + \gamma_d^{(0)}\right)\right] = \omega\int_0^\infty \frac{\mathcal{P}_d(\tau)}{\log(2)(1+\tau)}\mathrm{d}\tau,$$
(30)

$$\overline{\mathcal{C}}_{\min}^{(0)}(M) \triangleq \mathbb{E}\left[\mathcal{C}_{\min}^{(0)}(M)\right]$$
$$\approx \omega\mathbb{E}\left[\log_2\left(1 + \gamma_b^{(M')}\right)\right]$$
(31)
$$= \omega\int_0^\infty \frac{\mathcal{P}_b^{(M')}(\tau)}{\log(2)(1+\tau)}\mathrm{d}\tau.$$
(32)

$$P_1(M) \approx 1 - \mathbb{E}_{\gamma_d^{(0)}}\left[\mathcal{P}_b^{(M')}\left(\left(1 + \gamma_d^{(0)}\right)^{\nu^\star} - 1\right)\right](33)$$

$$P_2(M) \approx \mathbb{E}_{\gamma_d^{(0)}}\left[\mathcal{P}_b^{(M')}\left(\left(1 + \gamma_d^{(0)}\right)^{\nu^\star} - 1\right)\right]$$
$$- \mathbb{E}_{\gamma_d^{(0)}}\left[\mathcal{P}_b^{(M')}\left(\gamma_d^{(0)}\right)\right],$$
(34)

$$P_3(M) \approx \mathbb{E}_{\gamma_d^{(0)}}\left[\mathcal{P}_b^{(M')}\left(\gamma_d^{(0)}\right)\right].$$
(35)

for some M' that monotonically depends on M.

Proof: See Appendix D. ∎

Remark 7. *When $M \to \infty$, $\overline{\mathcal{C}}_{\min}^{(0)} \to 0$. Thus, $P_1(M) \to 1$ and $\mathbb{E}[\mathcal{R}_d] = \overline{\mathcal{C}}_d^{(0)}\nu^\star$, i.e., the mean DL rate is directly proportional to $\nu^\star$. In the general case, for a fixed M, $\mathbb{E}[\mathcal{R}_d]$ is an increasing function of $\nu^\star$.*

Remark 8. *For $\nu^\star = 1$, $\mathbb{E}[\mathcal{R}_d] = \overline{\mathcal{C}}_d^{(0)}$, which is independent of M and equivalent to the maximum achievable DL rate under our setting. This reaffirms the fact that there is no degradation on the DL when $\nu^\star = 1$.*

Lemma 2 (Average UL rate). *For all BS $x \in \Phi$, $\mathcal{R}_u(x) = \mathcal{C}_u(x; \mathcal{U}(x))$. Then, $\mathbb{E}[\mathcal{R}_u] = \overline{\mathcal{C}}_u^{(0)} = \omega\int_0^\infty \mathcal{P}_u(\tau)/(\ln(2)(1 + \tau))\,\mathrm{d}\tau$.*

V. SIMULATION AND PERFORMANCE EVALUATION

In this Section, we study the performance of the proposed model under realistic network parameters and we validate the assumptions made to derive the mathematical model, i.e.: • The scheduled UL and DL UEs locations are modeled by homogeneous PPPs of intensity λ; In simulations, DL and UL UEs are drawn uniformly in the Voronoi cell of every BS. • The point process of interfering BSs of a typical BS is given by thinning Φ according to the probability $p(r)$ of retaining a point at a distance r; In simulations, the sets I_M and J are built according to Algorithm 1. • $\mathcal{C}_{\min}(M)$ is approximated by $\mathcal{C}_b^{(M')}$ for some mapping between M and M'; In simulations, we compute exactly $\mathcal{C}_{\min}(M)$. • Antenna gains between equipments are calculated by computing average gains.

A. Simulation Settings

We simulate a network according to the values of Tab. II, which are based on the urban micro-cell (UMi) model with NLOS channels in [38], [39]. The values of $(\kappa, \tilde{\kappa}, \breve{\kappa})$ and $(\eta, \tilde{\eta}, \breve{\eta})$ are calculated by using the UMi-NLOS path-loss expression in [39, Section 7.4], i.e., $35.3\log_{10}(r) + 22.4 + 21.3\log_{10}(f_c) - 0.3(h_{Rx} - 1.5)$, where h_{Rx} is the receiver height. It is important to highlight that the UMi-NLOS path-loss model is also considered for BS-to-BS links. This is due to the fact that SC BSs are usually deployed below roof tops. A similar assumption is done in [10]. As seen in [5], [13], omnidirectional antennas at BSs represent a worst case scenario for FD deployments, since the co-channel interference is high in this type of networks. This is specially harmful, as the BS-to-BS interference critically impacts the UL performance. We thus take as a reference the assumption of omnidirectional antennas to validate our mathematical development and analyze the effectiveness of our algorithm. We then depart from the omnidirectional antenna assumption and assume beamforming in Section V-F. For this case, we use as benchmark the antenna parameters of BSs in [13], i.e., $G_d^{(\max)} = 20$ dBi, $G_d^{(\min)} = -10$ dBi and $\theta_{3\mathrm{dB}} = 30°$, as seen in Tab. II.

B. Model Validation

The BS-to-BS SINR CCDF as computed in (16) is shown in Fig. 3. Although we observe a small gap for $n = 1$, results match well for values of $n > 1$, validating the assumptions regarding the position of active UEs and the independence between the interference generated by UL users and BSs. Moreover, we observe that the performance decreases with n, which is intuitive as the distance between BSs is increasing.

TABLE II
GENERAL SIMULATION PARAMETERS

Parameter	Value	Parameter	Value	Parameter	Value	Parameter	Value
f_c	3.5 GHz	W	100 MHz	ω	360 kHz	R_c	100 m
Noise density	-174 dBm/Hz	Noise figure	8 dB	UE height	1.5 m	BS height	10 m
P_u	23 dBm	G_u	0 dBi	P_d	30 dBm	β	-110 dB
$G_d^{(\max)}$	20 dBi	$G_d^{(\min)}$	-10 dBi	$\theta_{3\text{dB}}$	$30°$	(κ, η)	$(9.18, 3.53)$
$(\breve{\kappa}, \breve{\eta})$	$(7.77, 3.53)$	$(\tilde{\kappa}, \tilde{\eta})$	$(9.18, 3.53)$				
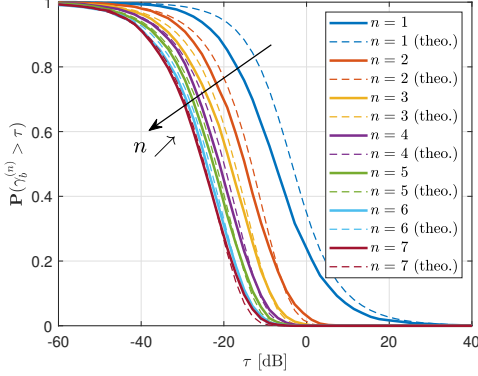
Fig. 3. BS-to-BS coverage probability.
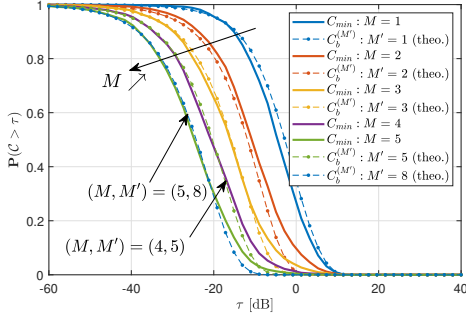
Fig. 4. Mapping between $\mathcal{C}_{\min}(M)$ and $\mathcal{C}_b^{(M')}$.

(a) $\nu^\star = 0$.

(b) $\nu^\star = 0.1$.

Fig. 5. Probability $p(r)$ for a BS to be not decodable at a distance r.

Fig. V-B shows the distribution of $\mathcal{C}_{\min}(M)$, obtained by simulations and the theoretical value of $\mathcal{C}_b^{(M')}$ (using (16)). We notice that theory and simulations match well for each pair M and M'. Particularly, when $M \leq 3$, it holds that $M' = M$. However, for greater values of M, e.g. for $M = \{4, 5\}$, we have that $M' > M$. This is due to the fact that the set $J(x; M)$ has a cardinality greater than M with increasing probability.

In Fig. 5, we plot $p(r)$, the probability for a BS to be not decodable at distance r, for two values of $\nu^\star$. When $\nu^\star = 0$, theory and simulation match very well. For $\nu^\star = 0.1$, a higher gap is observed for $M \geq 4$. Values of M higher than 4 are difficult to achieve because of the limitations of SIC due to decoding complexity and error propagation [36]. Most theoretical studies assume that M is not more than 4 or 5, see e.g. [40], [41] and all testbed implementations assume $M = 1$, see e.g. [42], [43]. For large values of M, a better accuracy can however be obtained by fitting $p(r)$ with a sigmoid function $1/(1 + \exp(-a(r - c)))$, where a and c are constants. As expected, $p(r)$ increases with r and decreases

with M because the probability for a BS to be among the M-th nearest neighbors decreases with r and increases with M.

The comparison between simulation and analysis for the UL coverage probability is shown in Fig. 6a and 6b. For $\nu = 0.01$ and $M = 5$, we have used the fitting of $p(r)$. For different values of M and ν, results match well. The conclusion is the same for the DL coverage probability in Fig. 6d.

C. Impact of $\nu^\star$ and M

Fig. 7a shows the mean UL data rate as a function of M for different values of $\nu^\star$. First, we see that FD (i.e., $M = 0$) has a performance 38% lower than that of HD. Then, we notice that the UL data rate increases when $\nu^\star$ decreases, since a higher loss is allowed on the DL. For very low values of $\nu^\star$, e.g. $\nu^\star \leq 0.06$ it is possible to outperform the HD performance. Hence, the HD UL data rate does not act as an upper bound when implementing our solution. We can also observe that even for a $\nu^\star = 1$, which is the value that obtains the lower gains, the FD UL rate is also outperformed. If we set $M = 4$
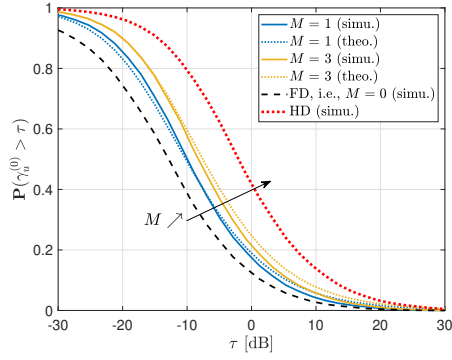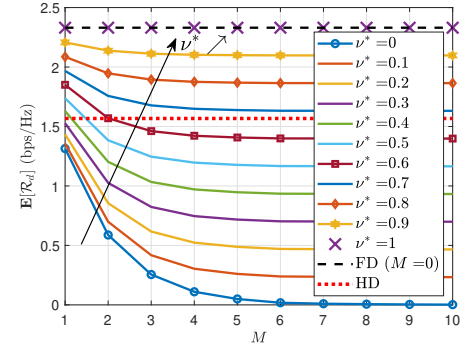
(a) UL coverage probability for $\nu^\star = 0$.
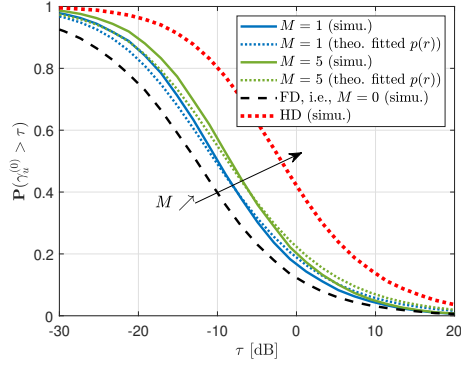
(b) UL coverage probability for $\nu^\star = 0.1$.
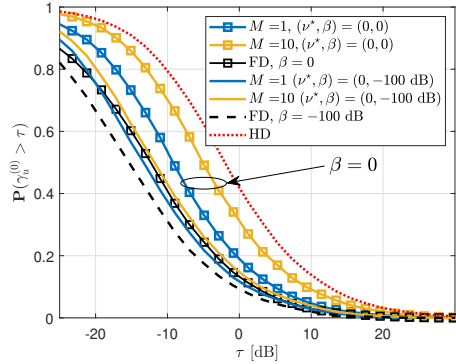
(c) UL coverage probability for different β's.
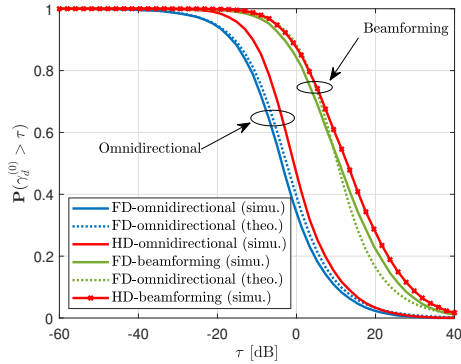
(d) DL coverage probability.

Fig. 6. Coverage probabilities: (a) UL for $\nu^\star = 0$, (b) UL for $\nu^\star = 0.1$ and $p(r)$ fitted with sigmoid function, (c) UL for different RSI values, (d) DL for BSs with omnidirectional and beamforming-capable antennas.
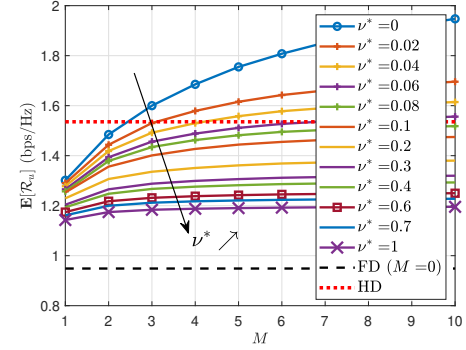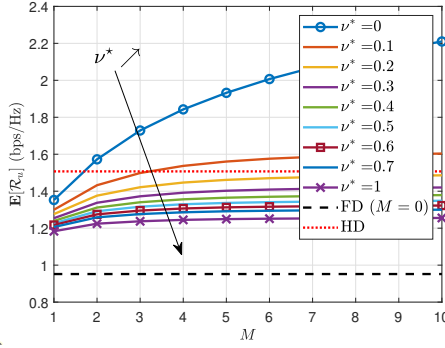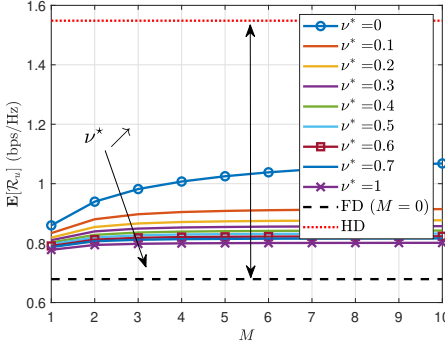

(a) Mean UL rate.

(b) Mean DL rate.

Fig. 7. Mean UL and DL rates as a function of M, for different values of $\nu^\star$, with omnidirectional antennas and $\beta = -110$ dB.

and $\nu^\star = 1$, we achieve a 25% gain with respect to FD and reduce the loss from 38% to 23% when compared to HD. On the other hand, we observe that the UL performance improves when M increases. Even for $M = 1$, our solution outperforms the traditional FD case. Indeed, if we consider $M = 1$ and $\nu^\star = 0.6$ we obtain a 24% gain with respect to FD and the loss compared to HD is reduced to 23%. For a fixed value of $\nu^\star$, the UL gains become marginal as M increases. This allows us to pick low values of M without considerably achieving lower performance gains. Indeed, due to SIC error propagation constraints, M cannot be chosen arbitrarily large [36]. Hence, we could in fact operate with values of $M = 2$ and $\nu^\star = 0.6$, increasing the FD performance by approximately 30%.

In Fig. 7b, we show the DL rate as a function of M and ν^*. We clearly see that, contrary to UL, the DL data rates are decreasing. Note first that traditional FD ($M = 0$) increases by 49% the performance of HD. Then, we notice that low values of $\nu^\star$ critically impair the DL rate. It is possible to surpass the HD performance for higher values of $\nu^\star$, namely $\nu^\star \geq 0.7$, independently of M. On the contrary, the FD DL rate is an upper bound. At last, the DL rate decreases with M. Our solution can however outperform the HD case even for $M = 1$. For example, when $M = 1$ and $\nu^\star = 0.6$, we obtain a 18% gain with respect to HD. Although UL and DL performance behave in the opposite way with respect to $\nu^\star$ and M, it is not required to trade UL for DL gain as in [2], [3], [5]. Indeed, setting $\nu^\star = 1$ and $M = 4$ allows us to maintain the performance of FD DL (i.e., 49% gain with respect to HD), while enhancing the FD UL by 25% and satisfying the

(a) Mean UL rate for perfect self-IC ($\beta = 0$).

(b) Mean UL rate for $\beta = -100$ dB.

Fig. 8. Mean UL rates for different RSI values (i.e., β) with omnidirectional antennas.

SIC constraints.

D. Impact of Residual Self-Interference

Fig. 6c shows the impact of β on the UL coverage probability for different values of M. Two values are considered: perfect self-IC ($\beta = 0$) and poor self-IC ($\beta = -100$ dB). As expected, a more efficient self-IC improves the UL performance. More surprisingly, the gain is higher with our solution ($M = 1$ or 10) than with traditional FD ($M = 0$). For $\beta = 0$ and $M = 10$ for example, we have a 8.2 dB gain compared to FD. This makes the performance close to HD.

The average UL rate is shown in Fig. 8a and 8b for $\beta = 0$ and -100 dB respectively. These figures should be compared to Fig. 7a obtained with $\beta = -110$ dB. As β decreases, the gap between FD and HD decreases to a lower bound obtained for $\beta = 0$. When β is large (Fig. 8b), it is not possible for our solution to outperform HD. When β gets smaller (Fig. 7a and 8a), it is possible to outperform HD with higher values of $\nu^\star$, i.e., less DL degradation. With $\beta = 0$ (perfect self-IC) and $\nu^\star = 1$ (no DL degradation with respect to FD) and $M = 4$, we outperform FD by a 31% (compared to 25% with $\beta = -110$ dB and 18% with $\beta = -100$ dB).

We summarize in Tab. III some recommended configurations of our solution under different values of β. Case (a) represents a FD network. In Case (b), the FD DL gain is maintained, the FD UL is enhanced while practical constraints of SIC are satisfied. This is arguably the best configuration. Case (c) is an intermediate setting that has a similar behavior

to (b). Nevertheless, SIC is only performed along one interfering BS and DL degradation is allowed ($\nu^\star = 0.6$). Thus, this case is especially useful when high SIC computing capabilities are not available.

E. CRAN implementation

In a CRAN topology, a CU runs our algorithm on behalf of BSs, so that every BS $x \in \Phi$ can cancel all interfering BSs $x' \in I_M(x)$ and, simultaneously, set $\nu(x) = 1$. Hence, for the DL rate, we achieve the performance of $\nu^\star = 1$ in Fig. 7b, and for the UL rate, the performance of $\nu^\star = 0$ in Fig. 7a. Therefore, with a CRAN and $M = 4$, our solution enables to outperform HD by 10% and FD by 78% in terms of UL rate, while maintaining the FD DL rate.

Note that DL transmit power control is also a solution allowing to balance the DL and UL performance. However, at any fixed downlink transmit power, the proposed solution outperforms the performance achieved by a FD network. DL power control can thus be used in conjunction with our scheme.

Case (d) in Tab. III summarizes the performance achieved by our solution for different values of β, when setting $M = 4$ and having a CRAN topology.

### F. Impact of antenna directivity

The mean UL and DL rates when using the two-lobe antenna model can be found in Fig. 9. For the UL (Fig. 9a), we observe that our system performs similarly as for the omnidirectional case, i.e., the UL rate is enhanced when $\nu^\star$ decreases and M decreases. However, and as before, the gains become marginal for greater values of M. Moreover, we notice that now the performance of FD is only 4% lower than the one of HD. Hence, with beamforming, FD does not experiences a critical UL degradation. As a consequence, our solution still enables an improvement compared to FD, but the gains are not substantial because the room of improvement is small.

VI. CONCLUSIONS

In this paper, we propose and study a base station coordination scheme based on successive interference cancellation aiming at mitigating the uplink degradation observed in full duplex cellular networks. The algorithm is characterized by two parameters, M and $\nu^\star$. The former represents the maximum number of base stations whose signal can be eventually suppressed by a receiver; the latter controls the maximum allowable resulting data rate reduction on the downlink. The performance depends on the architecture of the radio access network. In a centralized architecture, the solution outperforms classical full duplex networks by 78% on the uplink without affecting the downlink. In a distributed architecture, the gain can reach 25% without affecting the downlink. If a decrease of the downlink data rate is tolerated (controlled by the parameter $\nu^\star$), higher gains can be achieved. Numerical results show that the model is promising in scenarios, in which full duplex uplinks are critically degraded. This is particularly the case when base stations and user equipment have omnidirectional antennas.

TABLE III
UL AND DL DATA RATE GAINS WITH RESPECT TO HD AND FD NETWORKS. (A) FD NETWORK; (B) AND (C) PROPOSED SOLUTION WITH DISTRIBUTED
ARCHITECTURE ; (D) PROPOSED SOLUTION WITH CRAN ARCHITECTURE.

	Solution: $(\nu^\star, M)$	UL						DL	
		$\beta = 0$		$\beta = -110$ dB		$\beta = -100$ dB			
		wrt HD	wrt FD	wrt HD	wrt FD	wrt HD	wrt FD	wrt HD	wrt FD
(a)	$(1, 0)$	-37%	-	-38%	-	-56%	-	$+49\%$	-
(b)	$(1, 4)$	-17%	$+31\%$	-23%	$+25\%$	-48%	$+18\%$	$+49\%$	0%
(c)	$(0.6, 1)$	-19%	$+28\%$	-23%	$+24\%$	-49%	$+16\%$	$+18\%$	-20%
(d)	$(-, 4)$	$+22\%$	$+94\%$	$+10\%$	$+78\%$	-35%	$+48\%$	$+49\%$	0%
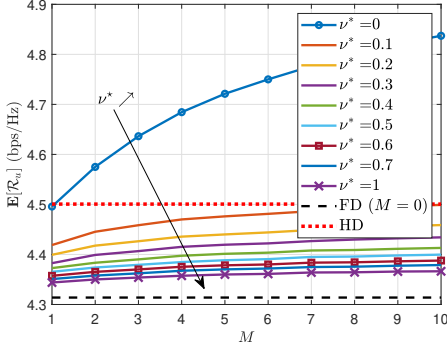
(a) Mean UL rate.
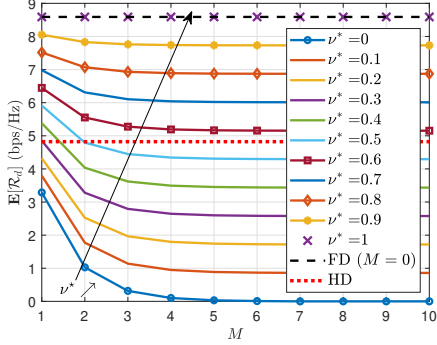
(b) Mean DL rate.

Fig. 9. Mean UL and DL rates as a function of M, for different values of $\nu^\star$, when considering directional antennas in BSs.

APPENDIX A

We use the approach in [32] to approximate the intensity of interfering UL users, Ψ_u, from the point of view of typical BSs and UEs. Here, the pair correlation function characterizes these intensities by inhomogeneous PPPs that depend on the distance to the typical equipment. From the point of view of a typical user, the intensity function of interfering UL users, at a distance r, can be approximated by $\lambda_u(r) = \lambda(1 - e^{-(9/4)\sqrt{\lambda}r} + 0.5\lambda r^2 e^{-(5/4)\lambda r^2})$. From the point of view of a typical BS, the intensity function of interfering UL users, at a distance r, can be approximated by $\lambda_u^{(\text{BS})}(r) = \lambda(1 - e^{-(13/2)\lambda r^2} + (2/7)\lambda r^2 e^{-(13/9)\lambda r^2})$. Then, the PDF of the distance between a BS and its served UE, R_0, is given by $f_{R_0}(r) = 2(13/10)\pi r\lambda \exp\left(-(13/10)\lambda\pi r^2\right)$.

Now, to compute the DL coverage probability, we condition upon the distance between the typical user and its BS, $R_0 = r$, and to the co-channel interference generated by ULs and DLs, i.e. $\mathbb{P}(\gamma_d^{(0)} > \tau | R_0 = r, I_{\text{BS}}^{(d)}, I_{\text{UE}}^{(d)})$, which can be developed

as:

$$\mathbb{P}\left(h > \frac{\tau(\kappa r)^\eta}{GP_d}\left[I_{\text{BS}}^{(d)} + I_{\text{UE}}^{(d)} + \sigma^2\right]\bigg|R_0 = r, I_{\text{BS}}^{(d)}, I_{\text{UE}}^{(d)}\right) =$$
$$\exp\left(-\frac{\tau(\kappa r)^\eta}{GP_d}\left[I_{\text{BS}}^{(d)} + I_{\text{UE}}^{(d)} + \sigma^2\right]\right) \quad (36)$$

where the equality comes from the Rayleigh fading, i.e., $h \sim \exp(1)$. Further, we assume that the interference generated by BSs is independent from the one from the UEs. Thus, by deconditioning with respect to $I_{\text{BS}}^{(d)}$ and $I_{\text{UE}}^{(d)}$ we obtain:

$$\mathbb{P}\left(\gamma_d^{(0)} > \tau | R_0 = r\right) =$$
$$\mathbb{E}_{I_{\text{BS}}^{(d)}}\left[\exp\left(-\frac{\tau(\kappa r)^\eta}{GP_d}I_{\text{BS}}^{(d)}\right)\right] \cdot$$
$$\mathbb{E}_{I_{\text{UE}}^{(d)}}\left[\exp\left(-\frac{\tau(\kappa r)^\eta}{GP_d}I_{\text{UE}}^{(d)}\right)\right] N_d(r, \tau),$$
$$= \mathscr{L}\{I_{\text{BS}}^{(d)}\}(r, \tau)\mathscr{L}\{I_{\text{UE}}^{(d)}\}(r, \tau)N_d(r, \tau). \quad (37)$$

Finally, we obtain (11) by integrating over the distribution of R_0. To derive the Laplace transforms, we neglect the effect of fast fading on the interference and replace it by its mean value [44, Section 2]. Thus, $\mathscr{L}\{I_{\text{BS}}^{(d)}\}$ can be written as:

$$\mathbb{E}\left[\exp\left(-\tau\frac{L_0}{GP_d}\sum_{x\in\Phi}\frac{G'P_d}{L(x)}\mathbb{1}\{\|x\| > r\}\right)\right] =$$
$$\mathbb{E}\left[\prod_{x\in\Phi}\exp\left(-\tau\frac{L_0G'}{L(x)G}\mathbb{1}\{\|x\| > r\}\right)\right], \quad (38)$$

where $L(x) = (\kappa' z)^{\eta'}$ ($z = \|x\|$ is the distance between an interfering BS located in x and the typical UE). Further, we use the property of the probability generating functional (PGFL) of a PPP ϕ, with intensity measure Λ, which states that [31, Sec. 4.6]: $\mathbb{E}[\prod_{w\in\phi} f(w)] = \exp\left(-\int_{\mathbb{R}}(1 - f(w))\Lambda(\text{d}w)\right)$ to obtain (13). We derive (14) by following similar steps.

APPENDIX B

Since Φ is a homogeneous PPP, the PDF of the distance between a typical BS and its n-th nearest neighbor is [45]: $f_R(r, n) = \frac{2(\pi\lambda)^n}{(n-1)!}r^{2n-1}e^{-\pi\lambda r^2}$. Now, the SINR between a typical BS and its n-th closest BS is: $\gamma_b^{(n)}(r) = \check{G}P_d h(r)L(r)^{-1}/(I_{\text{BS}}^{(n,1)} + I_{\text{BS}}^{(n,2)} + I_{\text{UE}}^{(b)} + I_{\text{RSI}} + \sigma^2)$, where r is the distance between these two elements, $L(r) = (\check{\kappa}r)^{\check{\eta}}$, $I_{\text{BS}}^{(n,1)}$ is the interference from the $n - 1$ BSs inside the disk of radius r, $I_{\text{BS}}^{(n,2)}$ is the interference from all BSs outside the latter disk and $I_{\text{UE}}^{(b)}$ is the interference from all scheduled UL

users. Similarly to the development in Appendix A we obtain that $\mathbb{P}(\gamma_b^{(n)}(r) > \tau \,|\, R = r)$ is:

$$\mathbb{P}(\gamma_b^{(n)}(r) > \tau \,|\, R = r) =$$
$$\mathbb{E}_{I_{\mathrm{BS}}^{(n)}}\left[\exp\left(-\frac{\tau\,L(r)}{\breve{G}P_d}I_{\mathrm{BS}}^{(n)}\right)\right]$$
$$\times \mathbb{E}_{I_{\mathrm{UE}}^{(b)}}\left[\exp\left(-\frac{\tau\,L(r)}{\breve{G}P_d}I_{\mathrm{UE}}^{(b)}\right)\right]N_b(r,\tau). \qquad (39)$$

Recalling that $I_{\mathrm{BS}}^{(n)} = I_{\mathrm{BS}}^{(n,1)} + I_{\mathrm{BS}}^{(n,2)}$, then the first expectation results in:

$$\mathbb{E}_{I_{\mathrm{BS}}^{(n,1)}}\left[\exp\left(-\frac{\tau\,L(r)}{\breve{G}P_d}I_{\mathrm{BS}}^{(n,1)}\right)\right]$$
$$\times \mathbb{E}_{I_{\mathrm{BS}}^{(n,2)}}\left[\exp\left(-\frac{\tau\,L(r)}{\breve{G}P_d}I_{\mathrm{BS}}^{(n,2)}\right)\right]. \qquad (40)$$

Further, we have that $I_{\mathrm{BS}}^{(n,1)} = \sum_{x \in \Phi}\breve{G}P_d L(x)^{-1}\mathbb{1}\{\|x\| < r\}$, where $\|x\|$ is the distance between an interfering BS and the typical BS. Let's denote $Z = \{z_1, \ldots, z_{n-1}\}$ the set of locations of the $(n-1)$ BS located in the disk of radius r. The first expectation of (40) reads:

$$\mathbb{E}_Z\left[\exp\left(-\tau\frac{L(r)}{\breve{G}P_d}\left(\frac{\breve{G}P_d}{L(z_1)} + \ldots + \frac{\breve{G}P_d}{L(z_{n-1})}\right)\right)\right] =$$
$$\prod_{i=1}^{n-1}\mathbb{E}_{Z_i}\left[\exp\left(-\tau\frac{L(r)}{L(z_i)}\right)\right]$$
$$= \left[\int_0^r \exp\left(-\tau\frac{(\breve{\kappa}r)^{\breve{\eta}}}{(\breve{\kappa}d)^{\breve{\eta}}}\right)\frac{2d}{r^2}\,\mathrm{d}d\right]^{n-1} \qquad (41)$$

where (41) is derived as all distances $\{z_1, \ldots z_{n-1}\}$ are i.i.d and distribute with PDF $P_Z(z) = 2z/r^2$ (uniform distribution of points inside a disk of radius r), from which we obtain (18).

Furthermore, $I_{\mathrm{BS}}^{(n,2)}$ can be written as: $I_{\mathrm{BS}}^{(n,2)} = \sum_{x \in \Phi}\breve{G}P_d L(x)^{-1}\mathbb{1}\{\|x\| > r\}$. Hence, the second expectation of (40) is expanded as in (38) and by performing the PGFL we obtain (19).

For the interference created by ULs, we can proceed similarly to the latter case and get $\mathscr{L}\{\prod I_{\mathrm{UE}}^{(b)}\}(r,\tau) = \mathbb{E}_\Phi[\prod_{y \in \Psi_u}\exp\left(-\tau\mu G(y)(\breve{\kappa}r)^{\breve{\eta}}/(\breve{G}(\kappa z)^\eta))\right)]$, where $G(y)$ is the antenna gain between the UL user in y and the typical BS. Then, we can apply the PGFL of the PPP of scheduled UL users. However, the closest UE which is at distance R_0 is the one served by the typical BS, thus the antenna gain between both elements is G. For other UEs, they are all farther than R_0 and their gains are G'. Consequently, by dividing the integral inside the expression resulting from the PGFL and taking the expected value with respect to R_0, we obtain (20). Finally, by integrating (39) over the distribution of $f_R(r,n)$, we obtain (16).

APPENDIX C

By considering Remark 4, we know that when $\nu^\star = 0$, it holds that $\mathcal{R}_d(r) \leq \mathcal{C}_b(r)$ and the typical BS can cancel the interference from all BSs in its set $I_M(\cdot)$. Hence we have in

(21) that: $\mathbb{P}(r \leq R_M \wedge \mathcal{R}_d(r) > \mathcal{C}_b(r)) = 0$ and we can write $p(r)$ in closed-form as:

$$\begin{aligned}
p(r) &= \mathbb{P}(r > R_M)\\
&= 1 - \int_r^\infty f_R(z, M)\mathrm{d}z = 1 - \frac{\Gamma(M, \lambda\pi r^2)}{(M-1)!}.
\end{aligned} \qquad (42)$$

In the general case, $p(r)$ can be further developed as:

$$\begin{aligned}
p(r) &= \mathbb{P}(r > R_M) + \mathbb{P}(r \leq R_M \wedge \mathcal{R}_d(r) > \mathcal{C}_b(r)),\\
&= \mathbb{P}(r > R_M) + \mathbb{P}(r \leq R_M)\\
&\quad \times \sum_{n=1}^\infty \mathbb{P}(\mathcal{R}_d(r) > \mathcal{C}_b^{(n)}(r)|n)\mathbb{P}(n-1) \qquad (43)\\
&= \mathbb{P}(r > R_M) + \mathbb{P}(r \leq R_M)\\
&\quad \times \sum_{n=1}^M \mathbb{P}(\mathcal{R}_d(r) > \mathcal{C}_b^{(n)}(r)|n \leq M)\mathbb{P}(n-1), \qquad (44)
\end{aligned}$$

where (43) is obtained by conditioning on the probability $\mathbb{P}(n-1)$ to have exactly $(n-1)$ BSs in the disk of radius r (which is a Poisson RV). Now note that by construction, there are only M BSs in the disk of radius R_M and thus there cannot be more than M BSs in the disk of radius $r \leq R_M$, we thus obtain (44). For a BS $x \in \Phi$, $\nu(x)$ can take three different values, described by the following events:

E_1: $\nu(x) = \nu^\star$; E_1 occurs when $\mathcal{C}_{\min}(x; M) < \mathcal{C}_d(x)$ and $\mathcal{C}_{\min}(x; M) \leq \nu^\star\mathcal{C}_d(x)$; in this case, $\mathcal{R}_d(r) = \nu^\star\mathcal{C}_d(r)$.

E_2: $\nu(x) = \frac{\mathcal{C}_{\min}(x;M)}{\mathcal{C}_d(x)}$; E_2 occurs when $\mathcal{C}_{\min}(x; M) < \mathcal{C}_d(x)$ and $\mathcal{C}_{\min}(x; M) > \nu^\star\mathcal{C}_d(x)$; in this case, $\mathcal{R}_d(r) = \mathcal{C}_{\min}(x; M)$.

E_3: $\nu(x) = 1$; E_3 occurs when $\mathcal{C}_{\min}(x; M) \geq \mathcal{C}_d(x)$; in this case, $\mathcal{R}_d(r) = \mathcal{C}_d(r)$.

For the typical BS located in 0, the probability of occurrence of each of these events is:

$$\mathbb{P}(E_1) \triangleq P_1(M) = \mathbb{P}\left(\mathcal{C}_{\min}^{(0)}(M) \leq \nu^\star\mathcal{C}_d^{(0)}\right), \qquad (45)$$

$$\mathbb{P}(E_2) \triangleq P_2(M) = \mathbb{P}\left(\nu^\star\mathcal{C}_d^{(0)} < \mathcal{C}_{\min}^{(0)}(M) < \mathcal{C}_d^{(0)}\right), \qquad (46)$$

$$\mathbb{P}(E_3) \triangleq P_3(M) = \mathbb{P}\left(\mathcal{C}_{\min}^{(0)}(M) \geq \mathcal{C}_d^{(0)}\right). \qquad (47)$$

We can now condition the probability in the sum of (44) with respect to these three events and obtain (48). Knowing that $n \leq M$ implies by definition that $\mathcal{C}_{\min}^{(0)}(M) \leq \mathcal{C}_b^{(n)}$, so that 'Term E_2'= 0. Again with the definition of $\mathcal{C}_{\min}^{(0)}(M)$, if $\mathcal{C}_{\min}^{(0)}(M) \geq \mathcal{C}_d(r)$, then necessarily $\mathcal{C}_b^{(n)} \geq \mathcal{C}_d(r)$, so that 'Term E_3'= 0. Finally, since we assume that PPPs of scheduled users and BSs are independent, we can consider that the DL capacity of the BS in r, i.e., $\mathcal{C}_d(r)$, has the same distribution as $\mathcal{C}_d^{(0)}$. Therefore, we write:

$$\begin{aligned}
&\mathbb{P}\left(\nu^\star\mathcal{C}_d(r) > \mathcal{C}_b^{(n)}(r)\right) =\\
&\quad \mathbb{P}\left(\nu^\star\log_2\left(1 + \gamma_d^{(0)}\right) > \log_2\left(1 + \gamma_b^{(n)}(r)\right)\right),\\
&= 1 - \mathbb{E}_{\gamma_d^{(0)}}\left[\mathscr{F}_b^{(n)}\left(r, \left(1 + \gamma_d^{(0)}\right)^{\nu^\star} - 1\right)\right], \qquad (49)
\end{aligned}$$

which provides the results.

$$p(r) = \mathbb{P}(r \le R_M) \sum_{n=1}^{M} \left[\underbrace{\mathbb{P}\left(\nu^\star \mathcal{C}_d(r) > \mathcal{C}_b^{(n)}(r) \middle| n \le M, \mathcal{C}_{\min}^{(0)}(M) \le \nu^\star \mathcal{C}_d(r)\right)}_{\text{Term } E_1} P_1(M) \right.$$

$$+ \underbrace{\mathbb{P}\left(\mathcal{C}_{\min}^{(0)}(M) > \mathcal{C}_b^{(n)}(r) \middle| n \le M, \nu^\star \mathcal{C}_d(r) \le \mathcal{C}_{\min}^{(0)}(M) \le \mathcal{C}_d(r)\right)}_{\text{Term } E_2} P_2(M)$$

$$+ \underbrace{\mathbb{P}\left(\mathcal{C}_d(r) > \mathcal{C}_b^{(n)}(r) \middle| n \le M, \mathcal{C}_{\min}^{(0)}(M) \ge \mathcal{C}_d(r)\right)}_{\text{Term } E_3} P_3(M) \left.\right] \frac{(\lambda \pi r^2)^{(n-1)}}{(n-1)!} e^{-\lambda \pi r^2} + \mathbb{P}(r > R_M). \quad (48)$$

APPENDIX D

Using the total expectation theorem it holds that

$$\mathbb{E}[\mathcal{R}_d] = \sum_i^3 \mathbb{E}[\mathcal{R}_d \mid E_i]\mathbb{P}[E_i]$$

$$= \nu^\star \omega \mathbb{E}[\log_2(1 + \gamma_d^{(0)})]P_1(M)$$
$$+ \mathbb{E}[\mathcal{C}_{\min}^{(0)}]P_2(M) + \omega \mathbb{E}[\log_2(1 + \gamma_d^{(0)})]P_3(M)$$
$$= \omega \mathbb{E}[\log_2(1 + \gamma_d^{(0)})](\nu^\star P_1(M) + P_3(M))$$
$$+ \omega \mathbb{E}[\log_2(1 + \gamma_b^{(M')})]P_2(M),$$

since we have assumed that $\mathcal{C}_{\min}^{(0)}(M) \approx \log_2(1 + \gamma_b^{(M')})$, and so $\mathbb{E}[\mathcal{C}_{\min}^{(0)}] \approx \omega \mathbb{E}\left[\log_2\left(1 + \gamma_b^{(M')}\right)\right]$. From the positivity of the SINRs, we can write: $\mathbb{E}[\log_2(1 + \gamma_m)] = \int_0^\infty \mathbb{P}(\log_2(1 + \gamma_m) > \tau)\mathrm{d}\tau = \int_0^\infty \mathbb{P}(\gamma_m > \tau)/(\ln(2)(1 + \tau))\mathrm{d}\tau$ to obtain (30) and (32).

REFERENCES

[1] H. A. Scharager, "Full-duplex for cellular networks: a stochastic geometry approach," Ph.D. dissertation, Institut Polytechnique de Paris, 2020.

[2] W. Tang, S. Feng, Y. Liu, and Y. Ding, "Hybrid Duplex Switching in Heterogeneous Networks," *IEEE Transactions on Wireless Communications*, vol. 15, no. 11, pp. 7419 – 7431, Nov. 2016.

[3] J. Lee and T. Q. S. Quek, "Hybrid Full-/Half-Duplex System Analysis in Heterogeneous Wireless Networks," *IEEE Transactions on Wireless Communications*, vol. 14, no. 5, pp. 2883 – 2895, May 2015.

[4] A. AlAmmouri, H. ElSawy, O. Amin, and M.-S. Alouini, "In-Band α-Duplex Scheme for Cellular Networks: A Stochastic Geometry Approach," *IEEE Transactions on Wireless Communications*, vol. 15, no. 10, pp. 6797–6812, Oct. 2016.

[5] H.-F. Arraño-Scharager, M. Coupechoux, and J.-M. Kelif, "Full and Half Duplex-Switching Policy for Cellular Networks under Uplink Degradation Constraint," in *IEEE International Conference on Communications*, May 2018.

[6] H. ElSawy, A. AlAmmouri, O. Amin, and M.-S. Alouini, "Can Uplink Transmissions Survive in Full-duplex Cellular Environments?" in *22th European Wireless Conference*, May 2016.

[7] Z. Zhang, K. Long, A. V. Vasilakos, and L. Hanzo, "Full-Duplex Wireless Communications: Challenges, Solutions, and Future Research Directions," *Proceedings of the IEEE*, vol. 104, no. 7, pp. 1369–1409, Jul. 2016.

[8] R. Li, Y. Chen, G. Y. Li, and G. Liu, "Full-Duplex Cellular Networks," *IEEE Communications Magazine*, vol. 55, no. 4, pp. 184–191, Apr. 2017.

[9] S. M. R. Islam, N. Avazov, O. A. Dobre, and K. sup Kwak, "Power-Domain Non-Orthogonal Multiple Access (NOMA) in 5G Systems: Potentials and Challenges," *IEEE Communications Surveys & Tutorials*, vol. 19, no. 2, pp. 721–742, 2017.

[10] J. Huang, K. Qi, Z. Xu, and C. Yang, "Hybrid Full and Half Duplex Networking," in *IEEE/CIC International Conference on Communications in China (ICCC)*, Jul. 2016.

[11] H. Tabassum, A. H. Sakr, and E. Hossain, "Analysis of Massive MIMO-Enabled Downlink Wireless Backhauling for Full-Duplex Small Cells," *IEEE Transactions on Communications*, vol. 64, no. 6, pp. 2354–2369, 6 2016.

[12] U. Tefek and T. J. Lim, "Full-Duplex Relaying in Machine-Type Communications with a Multi-Antenna Base Station," *IEEE Transactions on Wireless Communications*, vol. 17, no. 9, pp. 5804–5817, 9 2018.

[13] H.-F. Arraño-Scharager, J.-M. Kelif, and M. Coupechoux, "Performance Evaluation of Millimeter Wave Full-Duplex Cellular Networks," in *IEEE Global Communications Conference (GLOBECOM) Workshops: Full-Duplex Communications for Future Wireless Networks*, Dec. 2018.

[14] E. Everett, M. Duarte, C. Dick, and A. Sabharwal, "Empowering full-duplex wireless communication by exploiting directional diversity," in *Asilomar Conference on Signals, Systems and Computers*, 2011, pp. 2002–2006.

[15] C. Skouroumounis, C. Psomas, and I. Krikidis, "Heterogeneous FD-mm-Wave Cellular Networks with Cell Center/Edge Users," *IEEE Transactions on Communications*, vol. 67, no. 1, pp. 791–806, 1 2019.

[16] M. Wildemeersch, T. Q. S. Quek, M. Kountouris, A. Rabbachin, and C. H. Slump, "Successive Interference Cancellation in Heterogeneous Networks," *IEEE Transactions on Communications*, vol. 62, no. 12, pp. 4440–4453, Dec. 2014.

[17] X. Zhang and M. Haenggi, "The Performance of Successive Interference Cancellation in Random Wireless Networks," *IEEE Transactions on Information Theory*, vol. 60, no. 10, Oct. 2014.

[18] Z. Ding, P. Fan, and H. V. Poor, "On the Coexistence Between Full-Duplex and NOMA," *IEEE Wireless Communications Letters*, vol. 7, no. 5, pp. 692–695, Oct. 2018.

[19] M. Liu, Y. Mao, S. Leng, and K. Yang, "Successive Interference Cancellation in Full Duplex Cellular Networks," in *2017 IEEE International Conference on Communications (ICC)*, May 2017.

[20] S. Shahsavari, D. Ramirez, and E. Erkip, "Joint user scheduling and power optimization in full-duplex cells with successive interference cancellation," in *Asilomar Conference on Signals, Systems, and Computers*. IEEE, 2017, pp. 1099–1104.

[21] L. Huang, S. Han, C. Yang, and G. Wang, "Full-Duplex Based Successive Interference Cancellation in Heterogeneous Networks," in *2016 IEEE 27th Annual International Symposium on Personal, Indoor, and Mobile Radio Communications (PIMRC)*, Sep. 2016.

[22] X. Yue, Y. Liu, S. Kang, A. Nallanathan, and Z. Ding, "Exploiting Full/Half-Duplex User Relaying in NOMA Systems," *IEEE Transactions on Communications*, vol. 66, no. 2, pp. 560–575, Feb. 2018.

[23] M. F. Kader, S. Y. Shin, and V. C. M. Leung, "Full-Duplex Non-Orthogonal Multiple Access in Cooperative Relay Sharing for 5G Systems," *IEEE Transactions on Vehicular Technology*, vol. 67, no. 7, pp. 5831–5840, 2018.

[24] Zhengquan, Z. Ma, M. Xiao, Z. Ding, and P. Fan, "Full-Duplex Device-to-Device-Aided Cooperative Nonorthogonal Multiple Access," *IEEE Transactions on Vehicular Technology*, vol. 66, no. 5, pp. 4467–4471, May 2017.

[25] Z. Tong and M. Haenggi, "Throughput Analysis for Full-Duplex Wireless Networks with Imperfect Self-Interference Cancellation," *IEEE Transactions on Communications*, vol. 63, no. 11, pp. 4490–4500, 11 2015.

[26] I. Atzeni and M. Kountouris, "Full-Duplex MIMO Small-Cell Networks With Interference Cancellation," *IEEE Transactions on Wireless Communications*, vol. 16, no. 12, pp. 8362–8376, 10 2017.

[27] A. AlAmmouri, J. G. Andrews, and F. Baccelli, "A Unified Asymptotic Analysis of Area Spectral Efficiency in Ultradense Cellular Networks," *IEEE Transactions on Information Theory*, vol. 65, no. 2, pp. 1236–1248, Feb. 2019.

[28] J. G. Andrews, F. Baccelli, and R. K. Ganti, "A Tractable Approach to Coverage and Rate in Cellular Networks," *IEEE Transactions on Communications*, vol. 59, no. 11, pp. 3122 – 3134, Nov. 2011.

[29] J. M. B. da Silva, G. Fodor, and C. Fischione, "On the Spectral Efficiency and Fairness in Full-Duplex Cellular Networks," in *IEEE International Conference on Communications (ICC)*, May 2017.

[30] F. Baccelli and B. Błaszczyszyn, *Stochastic Geometry and Wireless Networks, Volume I - Theory*. Now Publishers, 2009.

[31] Martin Haenggi, *Stochastic Geometry for Wireless Networks*, 1st ed. Cambridge University Press, Nov. 2012.

[32] M. Haenggi, "User Point Processes in Cellular Networks," *IEEE Wireless Com. Let.*, vol. 6, no. 2, pp. 258–261, Apr. 2017.

[33] M. D. Renzo, "Stochastic Geometry Modeling and Analysis of Multi-Tier Millimeter Wave Cellular Networks," *IEEE Transactions on Wireless Communications*, vol. 14, no. 9, pp. 5038 – 5057, Sep. 2015.

[34] E. Everett, A. Sahai, and A. Sabharwal, "Passive Self-Interference Suppression for Full-Duplex Infrastructure Nodes," *IEEE Transactions on Wireless Communications*, vol. 13, no. 2, pp. 680–694, Jan. 2014.

[35] B. Błaszczyszyn, M. K. Karray, and H. P. Keeler, "Using Poisson processes to model lattice cellular networks," in *Proceedings IEEE International Conference on Computer Communications (INFOCOM)*, Apr. 2013, pp. 773–781.

[36] D. Tse and P. Viswanath, *Fundamentals of Wireless Communication*. Cambridge University Press, 2010.

[37] A. Goldsmith, *Wireless Communications*. Cambridge University Press, 2005.

[38] "Guidelines for Evaluation of Radio Interface Technologies for IMT-2020 (Report ITU-R M.2412-0)," International Telecommunication Union (ITU), Tech. Rep., Oct. 2017.

[39] "Technical Specification Group Radio Access Network; Study on channel model for frequencies from 0.5 to 100 GHz (TR 38.901 Release 16)," 3rd Generation Partnership Project (3GPP), Tech. Rep., Oct. 2019.

[40] L. Lei, D. Yuan, C. K. Ho, and S. Sun, "Power and channel allocation for non-orthogonal multiple access in 5g systems: Tractability and computation," *IEEE Transactions on Wireless Communications*, vol. 15, no. 12, pp. 8580–8594, 2016.

[41] L. Salaün, M. Coupechoux, and C. S. Chen, "Joint subcarrier and power allocation in noma: Optimal and approximate algorithms," *IEEE Transactions on Signal Processing*, vol. 68, pp. 2215–2230, 2020.

[42] D. Halperin, T. Anderson, and D. Wetherall, "Taking the sting out of carrier sense: interference cancellation for wireless lans," in *Proceedings of the 14th ACM international conference on Mobile computing and networking*, 2008, pp. 339–350.

[43] W. Cui, C. Liu, H. Mosavat-Jahromi, and L. Cai, "Sigmix: Decoding superimposed signals for iot," *IEEE Internet of Things Journal*, vol. 7, no. 4, pp. 3026–3040, 2020.

[44] G. George, "Device-to-Device Communication and Wearable Networks: Harnessing Spatial Proximity," PhD. Thesis, Universitat Pompeu Fabra, 2017.

[45] D. Moltchanov, "Distance Distributions in Random Networks," *Ad Hoc Networks*, vol. 10, no. 6, pp. 1146–1166, 2012.